



Differential scanning calorimetry response of aged NiTiHfPd shape memory alloys

Emre Acar¹ · Musa Çalışkan² · Haluk E. Karaca³

Received: 15 January 2019 / Accepted: 5 March 2019 / Published online: 7 March 2019
© Springer-Verlag GmbH Germany, part of Springer Nature 2019

Abstract

Phase transformation characteristics of an aged NiTiHfPd shape memory alloy were investigated through thermal cycling experiments via the differential scanning calorimetry technique. Effects of heating/cooling rate and thermal cycling on the phase transformation temperatures, enthalpies, and thermal hysteresis values were revealed. It was found that phase transformation temperatures and thermal hysteresis values alter considerably with thermal cycling. The transformation temperatures were found to be above 80 °C for all the heating rates, which makes this alloy a promising candidate for high-temperature applications in the selected aging conditions.

1 Introduction

Shape memory alloys (SMAs) are metallic smart materials that have current and promising potentials in many industries including medical, aerospace, building and construction in addition to electronics [1]. This potential originates from their unique ability to have reversible thermoelastic martensitic phase transformations. Due to this distinct behavior, two main properties of shape memory effect and superelasticity can be observed in shape memory alloys [1].

In experimental characterization of SMAs, differential scanning calorimetry (DSC) is an important technique to determine some shape memory properties including transformation temperatures (TTs), transformation enthalpies, and thermal hysteresis from the temperature-dependent heat flow curves [2]. Since it requires small samples for testing, DSC is generally one of the first methods utilized in experimental characterization of shape memory alloys.

NiTi alloys (Nitinol) are the most widely used SMAs in many industries owing to their excellent properties such as good mechanical strength and corrosion resistance in

addition to recoverable strain of 8–10% [1]. Thus, NiTi and NiTi-based alloys (NiTiHf, NiTiCu etc.) have been extensively studied by researchers up-to-date. For high-temperature (> 100 °C) applications, NiTiHf alloys have attracted great deal of attention due to their high TTs in addition to good functional properties [3, 4]. Besides high transformation temperatures, high strength is another concern for applications that requires high force and/or small and lightweight devices. Thus, studies have focused on developing new materials that have high TTs and high strength [5, 6]. NiTiHfPd alloy system has been one of the most promising high strength and high-temperature SMAs to date [5, 7, 8].

Shape memory properties of NiTiHfPd alloys have been investigated in both polycrystalline [5, 7, 8] and single crystal forms [9–12]. Superelastic behavior with reversible strain of up to 4% was observed even when compressive stress levels as high as 2 GPa were applied in the polycrystalline forms [5]. Moreover, it was revealed that [111]-oriented Ni_{45.3}Ti_{29.7}Hf₂₀Pd₅ single crystals can handle reversible strain of 2% under ultra-high stress of 1500 MPa [9]. Single crystal NiTiHfPd alloys can show full shape recovery at stress levels of up to 2.5 GPa, have a large superelastic temperature window (100 °C) and mechanical hysteresis (> 1200 MPa) [11]. On the other hand, TTs of NiTiHfPd alloys could be increased above 100 °C following by proper aging conditions [5]. Thus, NiTiHfPd alloys could be promising for high strength and high-temperature applications such as aerospace, automobile and oil–gas industry.

Besides high strength and high TTs, the phase transformation stability is an important requirement for SMAs

✉ Emre Acar
emreacar@erciyes.edu.tr

¹ Department of Aeronautical Engineering, Erciyes University, Melikgazi, 38039 Kayseri, Turkey

² Turkish Technic Services, Turkish Airlines, Bakırköy, 34149 Istanbul, Turkey

³ Department of Mechanical Engineering, University of Kentucky, Lexington, KY 40506, USA

since thermal cycling is an inevitable process in operation of devices designed using shape memory alloys. On the other hand, cycling rate is also important, because it gives idea in designing the most optimum version of an SMA for a specific application. The main objective of this study is to analyze the relationships between phase transformation characteristics (e.g., TTs, enthalpy, thermal hysteresis, etc.) and thermal cycling rates in aged $\text{Ni}_{45.3}\text{Ti}_{29.7}\text{Hf}_{20}\text{Pd}_5$ alloys through the DSC thermal analysis technique.

2 Experimental procedure

$\text{Ni}_{45.3}\text{Ti}_{29.7}\text{Hf}_{20}\text{Pd}_5$ polycrystalline shape memory alloys were manufactured by induction melting technique as casting of rods with diameter of 1" and length of 4". The alloys were homogenized at 1050 °C for 72 h followed by an extrusion process at a 7:1 ratio in diameter at 900 °C. It was previously found that NiTiHfPd alloys have the higher TTs if they are aged at around 650–700 °C. Since the focus was on their high-temperature behavior, the alloys were aged at 650 °C for 10 h in air followed by water quenching. The materials will be called "aged NiTiHfPd" throughout the manuscript for simplicity. The differential scanning calorimetry technique was used to capture heat flow curves in a Perkin-Elmer DSC Pyris 1 instrument. TTs were calculated

from the heat flow curves by the intersection method. The samples (in weight of 20–40 mg) were capsulated in disposable Perkin-Elmer or Thermal Support aluminum pans. Heating/cooling rate in the calorimetric measurements was selected to be 40 °C/min, 60 °C/min, and 80 °C/min to study the rate effects.

3 Results and discussion

Figure 1 shows the DSC results of the materials with thermal cycling rates of 40, 60, and 80 °C/min. The upper peaks (in blue color) show the austenite to martensite transformations via cooling, whereas the lower peaks (in red color) show the martensite to austenite phase transformations through heating. The transformation peaks are generally broad and transformation temperatures decreased with cycling for the all heating/cooling rates. It is clear that TTs above 80 °C were possible for the aged alloy.

Figure 2 shows the first thermal cycling DSC response of aged NiTiHfPd alloys for all the rates. It's clear that the transformation peaks were similar at the rates of 40 and 60 °C/min and they became sharper at the cycling rate of 80 °C/min. On the other hand, M_s temperature was observed to decrease as the cycling rate increased. M_s temperature was 150 °C for 40°C/min while it decreased to 142 °C for 80°C/

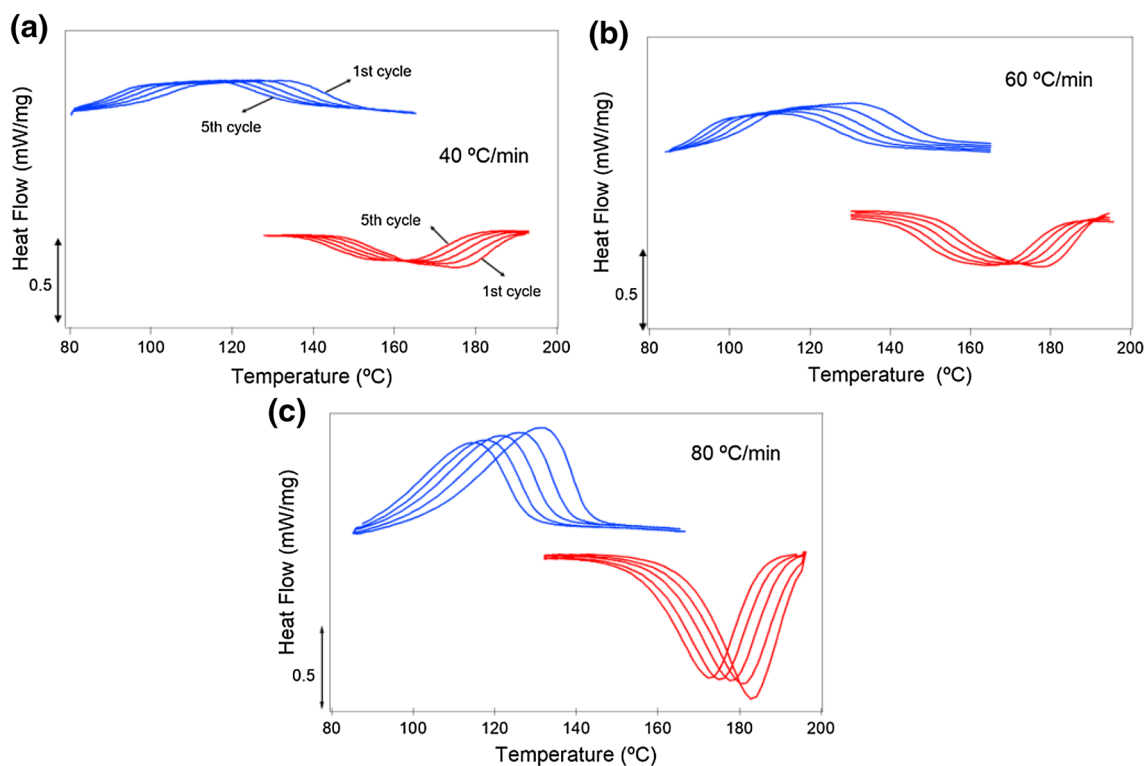


Fig. 1 DSC results of aged NiTiHfPd with thermal cycling rates of **a** 40 °C/min, **b** 60 °C/min, and **c** 80 °C/min

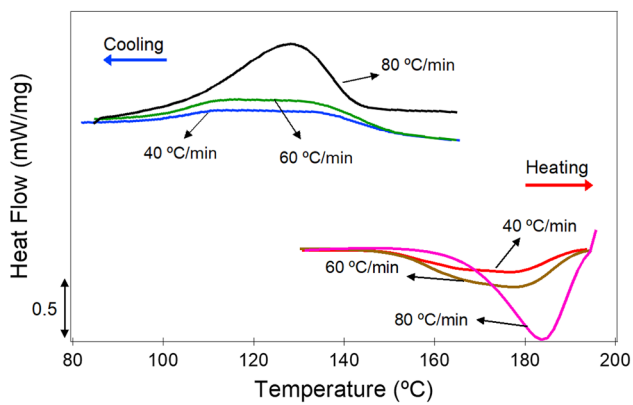


Fig. 2 DSC curves with heating/cooling rates of 40, 60, and 80 °C/min (note that the results belong to the first cycles for each cases for comparison)

min. It was also observed that M_s and A_s temperatures were comparable.

For the rate of 40 °C/min (Fig. 1a), the TTs of martensite finish (M_f), martensite start (M_s), austenite start (A_s) and austenite finish (A_f) temperatures were 98 °C, 153 °C, 149 °C, and 190 °C, respectively, in the first thermal cycle. The M_f , M_s , A_s and A_f were 99 °C, 150 °C, 149 °C, and 191 °C, respectively, in the first thermal cycle of thermal cycling rate of 60 °C/min. The measured TTs of the first cycle are 104 °C, 142 °C, 166 °C, and 194 °C for M_f , M_s , A_s , and A_f , respectively, for the rate of 80 °C/min.

Figure 3 shows the change in TTs (e.g., M_s and A_f) with cycling number. It is evident that TTs decreased with further thermal cycling for all the cycling rates.

The M_s temperatures were 153 °C and 142 °C for the cooling rates of 40 °C/min and 80 °C/min in the first cycles. It is clear that the temperature for the nucleation of martensite (e.g., M_s) shifted to lower temperatures with the increasing cooling rate. This is a similar phenomenon that was also observed in Ni₅₀Ti₅₀ shape memory alloys. It was observed that M_s temperatures of Ni₅₀Ti₅₀ alloys were

shifted to lower temperatures by increased cooling rates [13].

On the other hand, it was noted that the cycling has tangible effects on the TTs. For instance, the M_s temperature of the first cycle was 153 °C while it decreased to 135 °C after the fifth thermal cycle for the rate of 40 °C/min. For the same cycling rate, the A_f temperature decreased from 190 °C to 135 °C after five thermal cycles. Similar alterations were observed for the rest of the heating/cooling rates.

The decrease in the TTs could be explained by the hardening effect of dislocations generated in the microstructures during the thermal cycling process. It was previously reported that thermal cycling even under zero stress might cause dislocation generation in shape memory alloys [14]. Dislocations generated in the materials might hinder the motion of martensite phase front and consequently, extra energy might be required to start and complete the phase transformation [15]. This extra energy could be supplied by undercooling, ΔT . This behavior could be explained by the equation of $M_s = T_o - \Delta T$, where T_o is the thermodynamical equilibrium temperature. The decrease in TTs with cycling has been reported before [16] for many shape memory alloys including NiTi-based and Fe-based shape memory alloys [17, 18].

Figure 4 shows the change of first cycle TTs (e.g., M_s and A_f) with thermal cycling rates. The M_s decreased and the A_f slightly increased with increasing thermal cycling rate. The M_s temperatures were 153 °C and 142 °C for the cycling rates of 40 °C/min and 80 °C/min, respectively. On the other hand, the A_f temperatures were 180 °C and 184 °C for the cycling rates of 40 °C/min and 80 °C/min, respectively.

Figure 5 shows the thermal hysteresis calculated by ($A_f - M_s$) as functions of thermal cycling rate and cycle number. It is clear that hysteresis generally increased with increasing rate and cycle number followed by a saturation or decrease. This behavior of NiTiHfPd is different than what was observed in NiTi alloys. In NiTi alloys, thermal hysteresis was decreased with cycling and increased with rate [19].

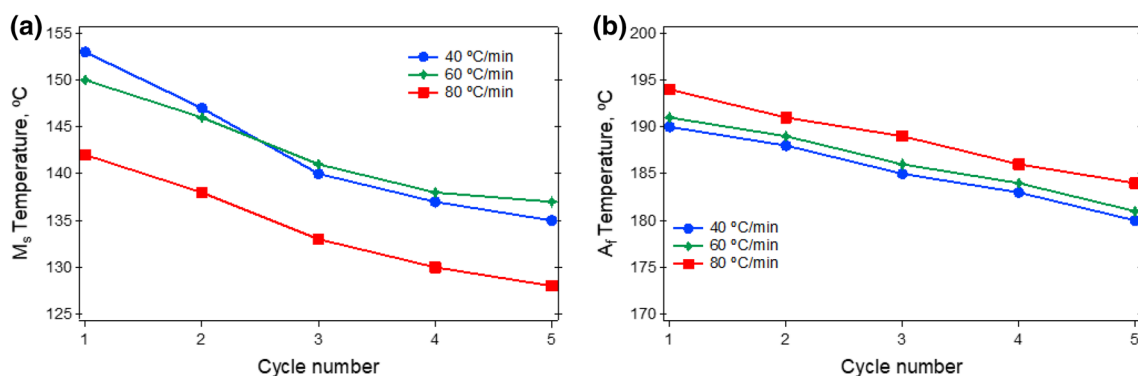


Fig. 3 Transformation temperatures as a function thermal cycling for the rates of 40 °C/min, 60 °C/min and 80 °C/min

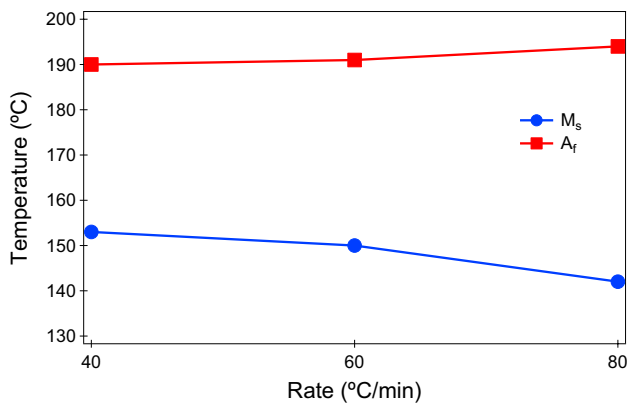


Fig. 4 Transformation temperatures as a function of heating/cooling rates

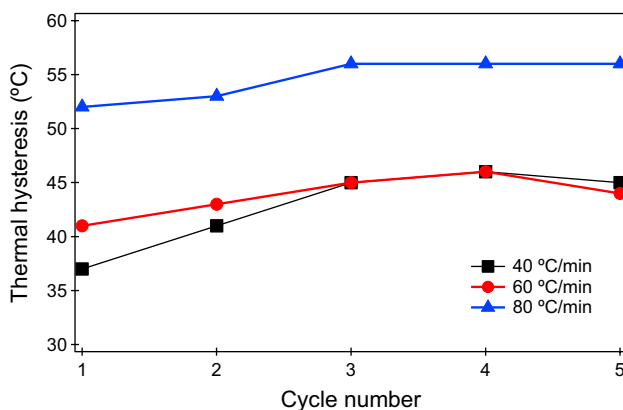


Fig. 5 Thermal hysteresis values as functions of thermal cycling rate and cycle number

It is widely known that hysteresis in SMAs originates from internal frictions. Possible internal friction mechanisms in SMAs could be stated as follows [20]:

1. Friction between austenite and martensite phase during phase transformation,
2. Friction between martensite plates,
3. Friction occurred between possible internal twins in martensite plates,
4. Friction between martensite phase and obstacles such as second phases, precipitates, defects, etc.

It is clear that thermal hysteresis as a result of energy dissipation increased with rate in the initial cycles in Fig. 5. Energy dissipation linked to the rate could be explained by the equation of $Q_{\max}^{-1} = K \frac{df}{dT} \frac{\dot{T}}{w}$ [21]. In this equation, K is a constant, $\frac{df}{dT}$ is the change of volume fraction of martensite with temperature, w is a shape change parameter and \dot{T} is the thermal cycling rate. Since $\frac{df}{dT}$ and w are only chemical

composition dependent, they should not change with rate or cycle number. Thus, \dot{T} is the decisive parameter in the abovementioned equation that could change considerable with rate or cycling. Based on this equation, energy dissipation and consequently, hysteresis should linearly increase with rate. Similar results have been reported for Ni_2MnGa [22] and $CuAlNi$ [23]. They also reported that internal friction increased as the cooling rates increased in those alloys.

On the other hand, thermal hysteresis generally increased with cycling number as shown in Fig. 5. A possible reason for this observation could be the generation/rearrangement of dislocations with cycling. As the dislocations are generated, energy dissipation could increase resulting in hysteresis in SMAs. The hysteresis tends to saturate or decrease after the fourth cycle. The reason behind this could be the saturation of dislocation density and consequently, energy dissipation due to dislocation density decreased in the alloys. Another possible reason for the decrease in the hysteresis could be the retained martensite in the microstructures with cycling. As the amount of material that could transform in each cycle decreases, lower hysteresis could be observed. Similar results have been reported for different alloy systems [24].

Another observation that gives idea about friction during transformation is the difference between A_f and M_s in Fig. 4. It is clear that the difference between A_f and M_s ($A_f - M_s$) increased with increasing cycling rate. The $A_f - M_s$ increased from 37 to 52 °C as the cycling rate increased from 40 to 80 °C/min. Based on this observation, it is possible to comment on thermal hysteresis of the alloys through the formulation of $\Delta G_{fr} = \frac{A_f - M_s}{2} \Delta S$ [25]. In this formula, ΔG_{fr} is the elastic energy relaxed due to friction (e.g., dissipation energy) and ΔS is the entropy change in phase transformation. According to the formula, as the $A_f - M_s$ increases, the friction energy also increases assuming the ΔS is constant. The increase in the friction energy means an increase in hysteresis, which was discussed earlier by experimental observations after Fig. 5.

Due to thermo-elastic martensitic transformation, shape memory properties have been modeled by many scientists up-to-date [26] using thermodynamics. Thermodynamical factors influencing the shape memory properties could be divided into chemical and non-chemical free energies [26]. Chemical energies include Gibbs free energies while the non-chemical energies include stored and released elastic energies [26]. Elastic energy storage and relief could directly affect the shape memory properties and energy dissipation, respectively. High elastic energy storage during the martensitic phase transformation could result in more gradual strain–temperature response in constant-stress thermal cycling experiments. On the other hand, hysteresis could increase as the stored energy released in SMAs [21]. The hysteresis shows the need of energy addition to complete

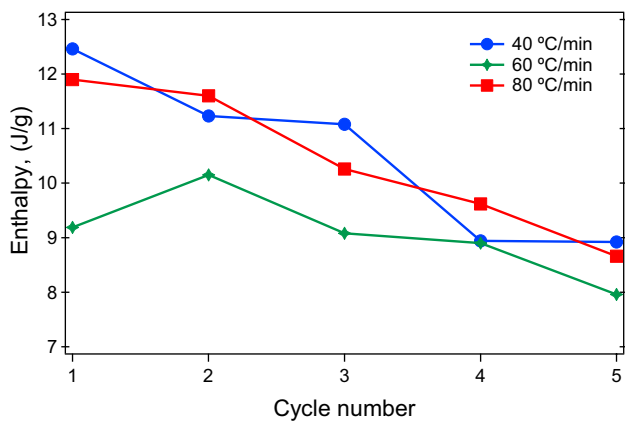


Fig. 6 Enthalpy values as a function cycle number and heating/cooling rates in NiTiHfPd alloys

phase transformation, which means that there is a resistance to shape change in SMAs [21].

Figure 6 shows the enthalpy values measured during martensite to austenite phase transformation as a function of thermal rate and cycle number. The enthalpy values were extracted from the DSC curves as shown in Fig. 1.

Transformation enthalpies were 12.5 J/g, 9.2 J/g and 11.9 J/g for the rates of 40 °C/min, 60 °C/min and 80 °C/min, respectively in the first cycle. The transformation enthalpies of binary NiTi alloys were reported to be in the range of 11–24 J/g for the $\text{Ni}_x\text{Ti}_{100-x}$ ($x=51\text{--}50.3$) alloys [27].

The enthalpies of aged NiTiHfPd alloys slightly decreased with cycling for all the cycling rates. A possible reason for the decrease in enthalpy could be a decrease in transformable material by cycling. As the material was thermally cycled, some dislocations could be generated in the microstructure. These dislocations could hinder austenite phase to completely transform to martensite and this forms retained austenite in the microstructure with cycling. Thus, volume fraction of transformed material decreases that results in a decrease in transformation enthalpy.

4 Conclusions

In this study, phase transformation characteristics of an aged NiTiHfPd shape memory alloy were investigated by analyzing the cyclic heat flow curves. Effects of heating/cooling rate and cycling on the phase transformation temperatures, enthalpies and thermal hysteresis were revealed. It was found that phase transformation temperatures and thermal hysteresis values were strong functions of thermal cycling. Transformation temperatures above 80 °C were possible for all the heating rates. M_s and A_f temperatures decreased after thermal cycling for all heating/cooling rates. On the other

hand, M_s temperatures were decreased while A_f temperatures were increased with heating/cooling rates. Thermal hysteresis values from 30 to 55 °C were observed in the experiments.

Acknowledgements This work was supported in part by the NSF CMMI-15-38665, the NASA EPSCoR program under Grant no: NNX-11AQ31A, KY EPSCoR RID program under Grant no: 3049024332, and Erciyes University under Grant no: FBA-2017-7604.

References

1. J.V. Humbeeck, Non-medical applications of shape memory alloys. *Mater. Sci. Eng. A* **134**, 273–275 (1999)
2. G. Airoidi, G. Riva, B. Rivolta et al., DSC calibration in the study of shape memory alloys. *J. Therm. Anal.* **42**, 781 (1994)
3. J. Ma, I. Karaman, R.D. Noebe, High temperature shape memory alloys. *Int. Mater. Rev.* **55**, 257 (2010)
4. H.E. Karaca, E. Acar, H. Tobe, M. Saghaian, NiTiHf-based shape memory alloys. *Mater. Sci. Technol.* **30**, 13a (2014)
5. H.E. Karaca, E. Acar, G.S. Ded, B. Basaran, H. Tobe, R.D. Noebe, G. Bigelow, Y.I. Chumlyakov, Shape memory behavior of high strength NiTiHfPd polycrystalline alloys. *Acta Materialia* **61**, 5036 (2013)
6. I. Kaya, H. Tobe, H.E. Karaca, E. Acar, Y. Chumlyakov, Shape memory behavior of [111]-oriented NiTi single crystals after stress-assisted aging. *Acta Metallurgica Sinica (English Letters)*, **29**(3), 282–286 (2016)
7. E. Acar, O.E. Ozbulut, H.E. Karaca, Experimental investigation and the modeling of the loading rate and temperature dependent superelastic response of a high-performance shape memory alloy smart *Mater. Struct.* **24**, 075020 (2015)
8. E. Acar, H. Tobe, I. Kaya, H.E. Karaca, Y.I. Chumlyakov, Compressive response of Ni_{45.3}Ti_{34.7}Hf₁₅Pd₅ and Ni_{45.3}Ti_{29.7}Hf₂₀Pd₅ shape memory alloys. *J Mater Sci* **50**, 1924 (2015)
9. H.E. Karaca, E. Acar, B. Basaran, R.D. Noebe, G. Bigelow, A. Garg, F. Yang, M.J. Mills, Y.I. Chumlyakov, Effects of aging on [111] oriented NiTiHfPd single crystals under compression. *Scripta Materialia* **67**, 728 (2012)
10. E. Acar, H.E. Karaca, B. Basaran, F. Yang, M.J. Mills, R.D. Noebe, Y.I. Chumlyakov, Role of aging time on the microstructure and shape memory properties of NiTiHfPd single crystals. *Mater. Sci. Eng. A* **573**, 161 (2013)
11. H.E. Karaca, E. Acar, B. Basaran, R.D. Noebe, Y.I. Chumlyakov, Superelastic response and damping capacity of ultra-high strength [111]-oriented NiTiHfPd single crystals *Scripta Materialia* **67**:447(2012)
12. E. Acar, H. Tobe, H.E. Karaca, R.D. Noebe, Y. Chumlyakov, Microstructure and shape memory behavior of [111]-oriented NiTiHfPd. alloys *Smart Materials and Structures* **25**(3), 035011 (2016)
13. S.H. Chang, S.K. Wu, Effect of cooling rate on transformation temperature measurements of Ti₅₀Ni₅₀ alloy by differential scanning calorimetry and dynamic mechanical analysis *Mater Character* **59**, 987 (2008)
14. C.M. Wayman, I. Cornelis, Transformation behavior and the shape memory in themally cycled TiNi *Scripta Metallurgica* **6**, 115 (1972)
15. N. Jost, E. Hornbogen, Influence of prior plastic deformation on the thermal- martensitic-transformation in an Fe-Ni-Al Alloy, *J Mater. Sci. Lett.* **6**, 491 (1987)

16. S. Besseghini, E. Villa, A. Tuissi, Ni-Ti-Hf shape memory alloy: effect of aging and thermal cycling. *Mater. Sci. Eng. A* **A273**, 390 (1999)
17. S. Miyazaki, Y. Igo, K. Otsuka, Effect of thermal cycling on the transformation temperatures of TiNi alloys. *Acta Metallurgica* **34**, 2045 (1986)
18. M.S. Andrade, R.M. Osthués, G.J. Arruda, The influence of thermal cycling on the transition temperatures of a Fe-Mn-Si shape memory alloy. *Mater. Sci. Eng. A* **512**, 273–275 (1999)
19. D.W. Berzins, H.W. Roberts, Phase transformation changes in thermocycled nickel–titanium orthodontic wires. *Dental Mater* **26**, 666 (2010)
20. H. Sehitoglu, R. Hamilton, H.J. Maier, Chumlyakov YI Hysteresis in NiTi alloys. *J Phys* **115**, 3 (2004)
21. F. Déborde, V. Pelosin, A. Rivière, Phase transformation in NiTi studied by isothermal mechanical spectrometry. *Scr. Metall. Mater.* **33**, 1993 (1995)
22. C. Seguí, E. Cesari, J. Pons, V. Chernenko, Internal friction behaviour of Ni–Mn–Ga. *Mater. Sci. Eng. A* **370**:481 (2004)
23. J. San Juan, M.L. Nó, Damping behavior during martensitic transformation in shape memory alloys. *J. Alloy. Compd.* **355**, 65 (2003)
24. H.E. Karaca, E. Acar, G.S. Ded, S.M. Saghaian, B. Basaran, H. Tobe et al., Microstructure and transformation related behaviors of a Ni_{45.3}Ti_{29.7}Hf₂₀Cu₅ high temperature shape memory alloy. *Mater. Sci. Eng.* **627**, 82 (2015)
25. E. Panchenko, Y. Chumlyakov, I. Kireeva, A. Ovsyannikov, H. Sehitoglu, I. Karaman, Effect of disperse Ti₃N₄ particles on the martensitic transformations in titanium nickelide single crystals. *Phys. Metals Metallogr* **106**:577 (2008)
26. P. Wollants, J.R. Roos, L. Dealey, Thermally and stress induced thermoelastic martensitic transformations in the reference frame of equilibrium thermodynamics. *Prog. Mater. Sci.* **37**, 227 (1993)
27. J. Khalil-Allafi, B. Amin-Ahmadi, The effect of chemical composition on enthalpy and entropy changes of martensitic transformations in binary NiTi shape memory alloys. *J. Alloys Compd.* **363**, 1–2 (2009)

Publisher's Note Springer Nature remains neutral with regard to jurisdictional claims in published maps and institutional affiliations.